

# Contribution of distribution network control to voltage stability: A case study

Petros Aristidou, *Student Member, IEEE*, Gustavo Valverde, *Member, IEEE*, and Thierry Van Cutsem, *Fellow Member, IEEE*

**Abstract**—A case study dealing with long-term voltage instability in systems hosting active distribution networks is reported in this paper. It anticipates future situations with high penetration of dispersed generation, where the latter are used to keep distribution voltages within desired limits, in complement to load tap changers. The interactions between transmission and active distribution networks are investigated on a 3108-bus test system. It involves transmission grid, large generators, and forty distribution networks, each with dispersed generation steered by a controller inspired of model predictive control. The reported simulations show the impact of distribution network voltage restoration as well as the benefit of load voltage reduction actuated by the dispersed generators.

**Index Terms**—Active distribution networks, voltage control, voltage stability, emergency control, load voltage reduction.

## I. INTRODUCTION

**S**MALL Dispersed Generation (DG) units operating at distribution level are expected to supply a larger and larger percentage of the demand [1], [2]. This proliferation of DGs and the advances in infocommunications are key drivers of the transformations seen today in Distribution Networks (DN).

The increased penetration of DG has given rise to new operational problems, such as over-voltages and thermal overloads at times of high DG production and low load. In response to these problems (and to the decommissioning of conventional plants connected to transmission grids), DG units will be requested to provide more ancillary services [3]. Furthermore, new and better coordinated schemes relying on modern communication infrastructure will be needed to control DG units. Such schemes are at the heart of smart grids. They offer an attractive alternative to expensive network reinforcement, as long as stressed operating conditions prevail for limited durations only. More specifically, this paper is devoted to Distribution Network Voltage (DNV) control.

This paper illustrates how DNV controllers can precipitate long-term voltage instability. The latter results from the inability of the combined transmission and generation system to deliver the power requested by loads [4], [5]. Traditionally, the driving force of instability is load power restoration through Load Tap Changers (LTCs) trying to restore DN voltages, and, hence, the load powers. At the same time, the maximum power that the transmission system can provide to loads is reduced by

OverExcitation Limiters (OELs) enforcing generator reactive power limits. The control of distribution voltages by DG units ignoring the weakening of the Transmission Network (TN) may accelerate long-term voltage instability, by adding to the load power restoration effect of LTCs.

On the other hand, since a higher controllability of DG units will be available, it is expected that distribution network operators will be requested to support transmission network operators in stressed operating conditions [6], [7]. As far as emergency voltage control is concerned, the DG units, being located close to the loads, offer additional flexibility to perform load voltage reduction. This well-known technique exploits the load sensitivity to voltage to decrease the demand [5], [8], [9]. Although not as effective as (under-voltage) load shedding [10], it may be applied as a first line of defense. The same technique, known as Conservation Voltage Reduction, is used to reduce peak demands and energy consumption [11], [12].

Traditionally, load voltage reduction is actuated through a reduction of the voltage set-points of LTCs controlling TN-DN transformers, and acting on a single distribution bus. This paper proposes a new scheme, complementing LTC voltage set-point reduction and acting on DG units. In normal conditions, the DG units are controlled to keep the voltages of various DN buses within a desired range. Once emergency conditions have been detected, the DG units are driven to bring the DN voltages to a lower range of values, while the LTC voltage set-point is decreased accordingly.

Moreover, many of the DN control developments are made assuming the presence of a strong TN, i.e. stiff transmission voltages. This assumption is no longer valid in degraded operating conditions, when interactions between transmission and distribution systems become critical. The results reported in this paper show that the behavior of DNV controllers are significantly affected in such cases.

The aforementioned harms and benefits of DNV control are demonstrated on a large-scale system involving a TN including multiple DNs with dispersed generation, all represented in detail. As the timing of controls is critical, long-term dynamic simulations were performed to simulate the system responses to large disturbances.

The remaining of the paper is organized as follows. Section II reviews the static aspects behind the voltage phenomena presented in the test cases. Section III describes the DNV control scheme and its coordination with the LTC. The test system is detailed in Section IV. Section V deals with the behavior in normal operating conditions, Section VI when voltage instability occurs, and Section VII when emergency

P. Aristidou is with the Dept. of Electrical Engineering and Computer Science, University of Liège, Belgium, email: [p.aristidou@ieee.org](mailto:p.aristidou@ieee.org)

G. Valverde is with the EPER Lab, School of Electrical Engineering at the University of Costa Rica, Costa Rica, email: [gvalverde@eie.ucr.ac.cr](mailto:gvalverde@eie.ucr.ac.cr)

T. Van Cutsem is with the Fund for Scientific Research (FNRS) at the University of Liège, Belgium, email: [t.vancutsem@ulg.ac.be](mailto:t.vancutsem@ulg.ac.be)

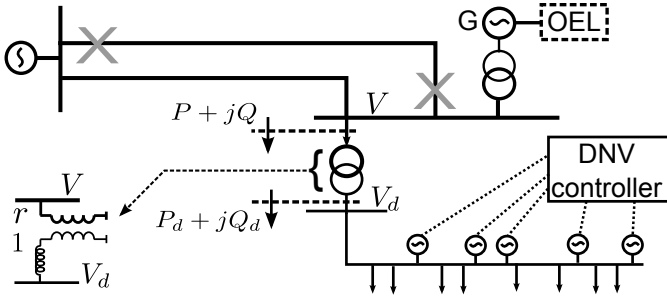


Figure 1. Simple system with DN controlled by LTC and DG units

support from DNs is implemented. The most salient points of the paper are summarized in Section VIII.

## II. IMPACT OF DNV CONTROL ON VOLTAGE STABILITY: BASIC STATIC ASPECTS

In this section, the basic mechanism of long-term voltage instability as related to maximum load power [5] is revisited, in the presence of DG in the distribution network.

Let us consider a DN feeding loads and hosting DG units, as shown in Fig. 1. The voltage on the TN and DN sides of the transformer are  $V$  and  $V_d$ , respectively. The complex power entering the transformer on the TN side is  $P + jQ$ , and leaving the transformer on the DN side  $P_d + jQ_d$ .

### A. Case of a passive DN

In traditional (passive) DNs, the DG units operate at constant active and reactive powers, i.e. they behave as constant power injectors. The loads, on the other hand, are sensitive to voltage and hence the net load power  $P_d + jQ_d$  can be considered a function of  $V_d$ .

The LTC is initially in steady state, with  $V_d$  equal to the setpoint value  $V_d^o$ . Let us consider an incident in the transmission system causing drops in both  $V$  and  $V_d$ . In response to this, the LTC will adjust the transformer ratio  $r$ , in successive steps, to restore  $V_d$  (close) to  $V_d^o$ . If these tap changes are successful, and assuming a negligible LTC deadband, the power on the distribution side is restored to the pre-disturbance value  $P_d(V_d^o) + jQ_d(V_d^o)$ . Using the transformer model in the lower left of Fig. 1, it is easily shown that  $P + jQ$  is also restored to its pre-disturbance value.

The voltage instability mechanism for this simple system can be conveniently depicted in the  $(P, Q)$  space of load powers [5], [13], as presented in Fig. 2. In the latter, there exists a feasible region, in which the combined generation and transmission system model has (at least) one equilibrium point. For load powers outside this region, the (algebraic) equations characterizing that system in steady state have no solution. Following the outage of a transmission and/or generation equipment, the feasible region shrinks.

Voltage instability occurs when the post-disturbance feasibility region is so much reduced that it no longer contains the point representing the restored load power. This is sketched in Fig. 2 with the boundary  $\Sigma$  of the post-disturbance feasibility shown with solid line and the restored load power with a

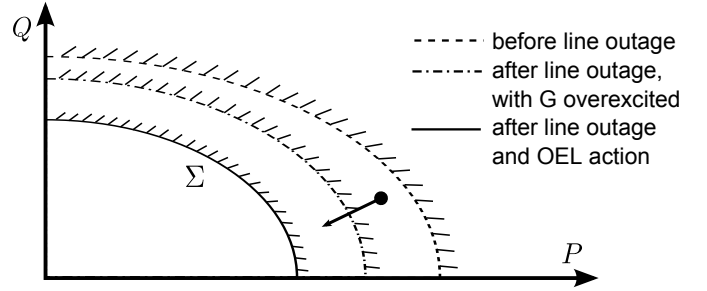


Figure 2. Feasible region in the load power space

black dot. After the line outage, the LTC will fail restoring the distribution voltage to  $V_d^o$  and, hence, the power  $P + jQ$  to its pre-disturbance value. These unsuccessful attempts make the transmission voltage  $V$  fall below an acceptable value.

Real-life systems are obviously more complex, with a load power space of much higher dimension. Furthermore, the limits on generator reactive power enforced by OELs, for instance, contribute to further shrinking the feasible region. For the simple system of Fig. 1, the feasible region, shown in Fig. 2, shrinks under the effects of the line outage followed by the reduction of the field current of generator  $G$  located next to the load.

As mentioned in the Introduction, load voltage reduction in passive DNs consists of decreasing  $V_d^o$ , and thereby the power consumed by the voltage-sensitive loads. As a result, the restored load power point can be moved as shown in Fig. 2. This approach is only effective if the point enters the post-contingency feasible region  $\Sigma$  (not the case in the shown figure).

### B. Case of an active DN

In this case, the DG units within a given DN are controlled with the objective of keeping the distribution voltages within a desired range. The units are assumed to operate at their maximum available active power, thus no more active power can be injected in the DN. Furthermore, a decrease of the injected active power is not considered during low TN voltage conditions, as it would increase the net load power  $P_d$ .

Thus, under the assumption that the TN voltage  $V$  remains almost constant, the DNV control will consist of increasing the DG unit reactive power productions when the monitored DN voltages fall below some lower limit, and conversely for high voltages. By controlling the voltages at DN buses other than the one controlled by the LTC, the DG units supplement the LTC. An algorithm to perform this task will be presented in Section III.

When considering mild TN disturbances, the DNV controllers can contribute to supporting DN voltages, with the possible benefit of reducing the number of LTC operations. An increase of DN voltages is obtained by increasing the reactive powers produced by DG units. This has two opposite effects. On one hand, the additional reactive power is exported to the TN, thus reducing the net load power  $Q$ . On the other hand, higher DN voltages cause increased consumption by the voltage-sensitive loads (both  $P$  and  $Q$ ).

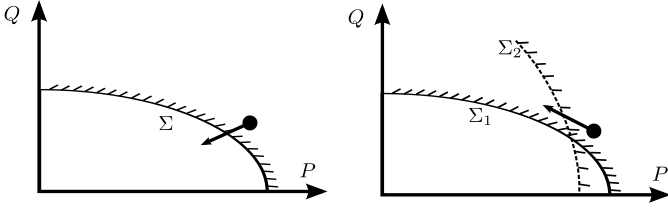


Figure 3. Load power space: DN voltage reduction by LTC and DG units

In voltage unstable scenarios, the DG units may amplify the detrimental effect of LTCs. Indeed, through their faster controlled electronic interfaces they may accelerate load restoration and the fall of TN voltages. However, they may also be used, jointly with the LTC, to perform load voltage reduction.

By reducing the DN voltages, the active power  $P$  will decrease, and due to the more extended control throughout the DN, that reduction is expected to be more pronounced. As regards the reactive power  $Q$ , the two antagonistic effects mentioned above have to be considered: the load reactive power will decrease with the DN voltages but, to decrease the DN voltages, the DG units have to reduce their reactive power productions. Thus, the net effect can be either an increase or a decrease of  $Q$ . Both possibilities are considered in Fig. 3.

In the left sub-figure of Fig. 3, it is assumed that both  $P$  and  $Q$  decrease by an amount sufficient to bring back the restored power point into the post-disturbance feasible region, thus restoring a long-term equilibrium and giving a chance to the system to be stabilized. In the right sub-figure, it is assumed that  $P$  decreases but  $Q$  increases. For a post-disturbance feasibility region with boundary  $\Sigma_2$  the system also recovers a long-term equilibrium, while for a region with boundary  $\Sigma_1$  it does not.

In Sections V to VII, the above mechanisms are supported by simulation results, including dynamic effects in addition to the static considerations presented so far.

### III. COORDINATED VOLTAGE CONTROL OF DG UNITS

The main features sought in this study for DNV control are:

- being able to regulate voltage at DN buses other than the one controlled by the LTC, and
- being able to steer the DG units progressively along a trajectory from the current to the desired operating point.

Although, any DNV controller complying with these requirements can be used to perform these studies (e.g. [14]), the Model Predictive Control (MPC) scheme in [15] was chosen. The latter dispatches the DG units in a centralized, coordinated and smooth manner.

In this study multiple instances of the same controller, each in charge of a DN, operate concurrently. That is, the scheme is centralized at DN level, yet distributed seen by the TN. In theory, this would require to exchange information and coordinate the control actions [16], [17]. However, since the DNs can only interact through the TN, that interaction is negligible as long as the TN voltages are stiffly controlled. On the contrary, in deteriorated TN conditions, it is necessary to adjust the DN control logic, as illustrated in Section V.

### A. Controls

In this study, it is assumed that a number of DNs have their voltages regulated by DNV controllers, each gathering real-time measurements in its DN and acting in a coordinated manner on the DG units of concern. As mentioned above, the controllers do not exchange information with each other.

In the general formulation of [15], the control variables are the active and reactive power set-points of the DG units:

$$\mathbf{u}(k) = [\mathbf{P}_g(k)^T \mathbf{Q}_g(k)^T]^T \quad (1)$$

where  $T$  denotes array transposition and  $k$  is the discrete time.

An obvious countermeasure against voltage instability consists of increasing the DG active powers, so as to reduce the net power drawn from the TN. This study, however, concentrates on load voltage control and all units are assumed to operate at their maximum available active power.

The DNV controller monitors the voltages at some DN buses and, if their measured values fall outside a specified range, it brings them progressively within the desired interval. Once this is achieved, the controller stops acting.

### B. Mathematical formulation

At time  $k$ , the controller uses a sensitivity-based model to predict the behavior of the system over a future interval with  $N_p$  discrete steps:

$$\begin{aligned} \mathbf{V}(k+i|k) &= \mathbf{V}(k+i-1|k) + \frac{\partial \mathbf{V}}{\partial \mathbf{u}} \Delta \mathbf{u}(k+i-1) \\ &+ \frac{\partial \mathbf{V}}{\partial V_{ctld}} \Delta V_d \gamma(k+i) \quad i = 1, \dots, N_p \end{aligned} \quad (2)$$

where  $\Delta \mathbf{u}(k) = \mathbf{u}(k) - \mathbf{u}(k-1)$  is the vector of control changes and  $\mathbf{V}(k+i|k)$  the one of predicted bus voltages at time  $k+i$  given the measurements at time  $k$ ,  $\mathbf{V}(k|k)$  is set to the measured values received at time  $k$ . Matrix  $\frac{\partial \mathbf{V}}{\partial \mathbf{u}}$  and vector  $\frac{\partial \mathbf{V}}{\partial V_{ctld}}$  contain the sensitivities of voltages to control variables and to the LTC-controlled voltage  $V_{ctld}$ , respectively.

An important aspect is the coordination between the controller and the LTC (if any). There are two options: either the LTC voltage set-point is included in the controls  $\mathbf{u}$ , or the LTC is left to act independently but the controller anticipates those actions [7], [15]. The latter option has been preferred in this study for its higher simplicity. It is implemented through the last term in Eq. (2), where  $\Delta V_d$  is the expected increase of the LTC-controlled voltage after one tap change, and  $\gamma(k)$  is a binary variable, equal to one if a tap change is anticipated at time  $k$ , and zero otherwise. When LTC actions are anticipated,  $N_p$  is increased to encompass in Eq. (2) the effect of all expected tap changes, as detailed in [15].

Using the latest available measurements, the controller determines an optimal sequence of  $N_c$  control changes  $\Delta \mathbf{u}(k), \Delta \mathbf{u}(k+1), \dots, \Delta \mathbf{u}(k+N_c-1)$ , where  $N_c \leq N_p$ . According to MPC principle [18], only the first control action  $\Delta \mathbf{u}(k)$  is applied. At the next time step, new measurements are acquired, a new sequence of  $N_c$  corrections is computed of which, again, only the first component is applied.

The sensitivities  $\frac{\partial \mathbf{V}}{\partial \mathbf{u}}$  and  $\frac{\partial \mathbf{V}}{\partial V_{ctld}}$  are computed using standard power-flow techniques. For details please refer to [7], [15].

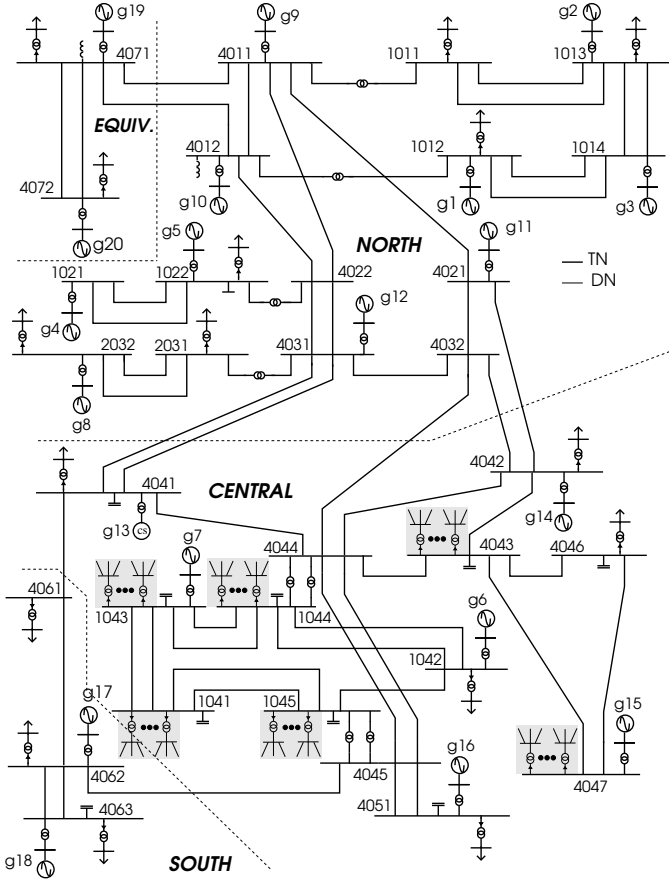


Figure 4. Nordic transmission test system with detailed DNs at six buses

The sequence of control changes optimizes a multi-time step objective under constraints. The following quadratic objective is considered at time  $k$ :

$$\min_{\Delta \mathbf{u}, \boldsymbol{\varepsilon}} \sum_{i=0}^{N_c-1} \|\Delta \mathbf{u}(k+i)\|_{\mathbf{R}}^2 + \|\boldsymbol{\varepsilon}\|_{\mathbf{S}}^2 \quad (3)$$

where the squared control changes aim at distributing the effort more evenly over the DG units and the time steps.  $\mathbf{R}$  is a weight matrix used to force control priorities. For example, higher costs are assigned to variations of  $\mathbf{P}_g$  compared to  $\mathbf{Q}_g$ . The slack variables  $\boldsymbol{\varepsilon} = [\varepsilon_1 \varepsilon_2]^T$  are used when some of the constraints, detailed hereafter, make the optimization problem infeasible. These variables are heavily penalized using the weight matrix  $\mathbf{S}$ , to keep them at zero when the problem is feasible.

The minimization is subjected to the equality constraints (2) as well as the following inequalities:

$$\mathbf{u}^{\min} \leq \mathbf{u}(k+i) \leq \mathbf{u}^{\max} \quad i = 0, 1, \dots, N_c - 1 \quad (4a)$$

$$\Delta \mathbf{u}^{\min} \leq \Delta \mathbf{u}(k+i) \leq \Delta \mathbf{u}^{\max} \quad i = 0, 1, \dots, N_c - 1 \quad (4b)$$

$$-\varepsilon_1 \mathbf{1} + \mathbf{V}^{\min} \leq \mathbf{V}(k+N_p|k) \leq \mathbf{V}^{\max} + \varepsilon_2 \mathbf{1} \quad (4c)$$

The constraints (4a) are associated with the permitted range of control variables. The active powers, updated from real-time measurements, are already at their upper limits. The reactive power limits are updated with the voltage and active power as described in [19], based on the information in [20] for the

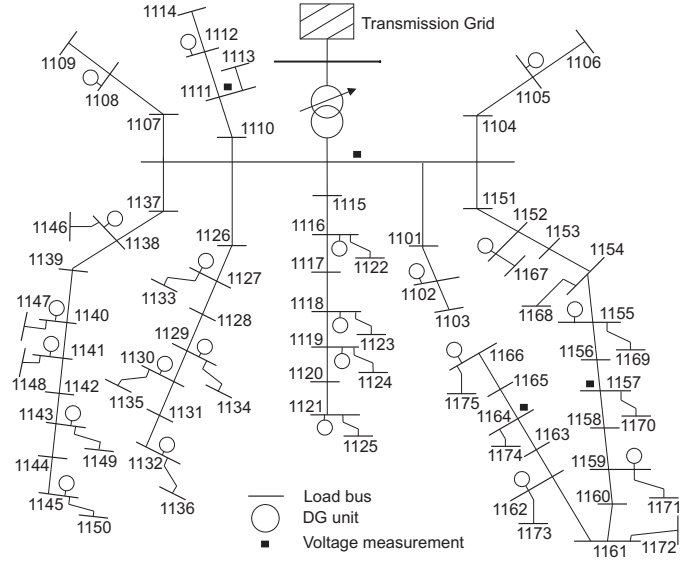


Figure 5. Topology of each of the 40 distribution networks

DFIGs. The constraints (4b) are associated with the rate of change of control variables. In inequalities (4c),  $\mathbf{1}$  denotes a vector of ones, while  $\mathbf{V}^{\min}$  (resp.  $\mathbf{V}^{\max}$ ) is the desired lower (resp. upper) limit on the voltages. Note that voltages are forced to reintegrate their limits at the prediction horizon, i.e. at time step  $k + N_p$  only. This MPC scheme, due to its closed-loop nature [18], accommodates inaccuracies incurred in (2), and the unpredicted changes in DG active powers [7].

In principle, the above control scheme is designed to control DN voltages only. The relation of the DNV control to TN voltage stability is established by the voltage limits  $\mathbf{V}^{\min}$  and  $\mathbf{V}^{\max}$  set in (4c). The selection of these limits can make a difference between reaching a new long term equilibrium point or not, as it will be shown in the following sections.

#### IV. TEST SYSTEM AND OVERVIEW OF SIMULATIONS

##### A. Network description

As mentioned in the Introduction, the case study was performed on a combined transmission and distribution model.

The TN part re-uses the Nordic test system currently investigated by the IEEE PES Task Force on Test Systems for Voltage Stability and Security Analysis. The variant considered is documented in [21]. Its one-line diagram is shown in Fig. 4. It includes 68 buses and 20 synchronous machines modeled with their excitation systems, voltage regulators, power system stabilizers, speed governors and turbines.

The original TN model included 22 aggregate, voltage-dependent loads behind explicitly modeled TN-DN transformers. Six of them were replaced by 40 detailed distribution systems, behind new TN-DN transformers of smaller powers, as sketched in Fig. 4. The six buses were chosen in the Central area because it is the most impacted by voltage instability.

Each DN is a replica of the same medium-voltage distribution system, whose one-line diagram is shown in Fig. 5. It consists of eight 11-kV feeders all directly connected to the TN-DN transformer, involving 76 buses and 75 branches. The

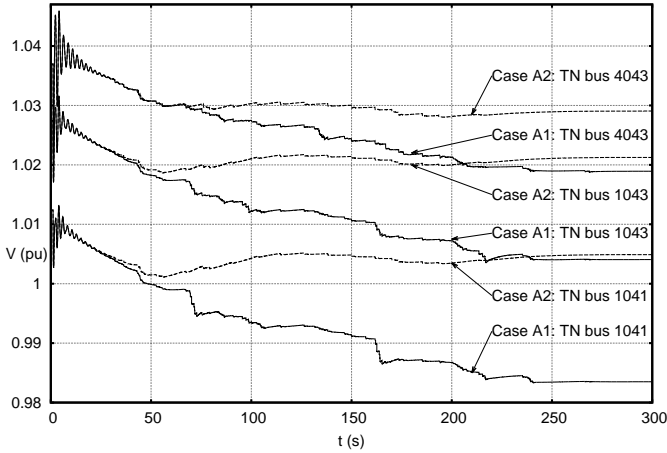


Figure 6. Cases A1 & A2: voltages at three TN buses

various DNs were scaled to match the original (aggregate) load powers, while respecting the nominal values of the TN-DN transformers and other DN equipment.

The transformer connecting each DN to the TN is equipped with an LTC controlling its distribution side voltage. To avoid artificial synchronization of transformers, the delays on tap changes were randomized around their original values. Thus, the first tap change takes place 28-32 s after leaving the voltage dead-band and the subsequent changes occur every 8-12 s.

Each DN serves 38 voltage sensitive loads and 15 represented by equivalent induction motors. The voltage sensitive loads are modelled as:

$$P = P_0 \left( \frac{V}{V_0} \right)^\alpha \quad Q = Q_0 \left( \frac{V}{V_0} \right)^\beta \quad (5)$$

with  $\alpha = 1.0$  (constant current) and  $\beta = 2.0$  (constant impedance), respectively.  $V_0$  is set to the initial voltage at the bus of concern, while  $P_0$  and  $Q_0$  are the corresponding initial active and reactive powers. The equivalent motors are representative of small industrial motors, with constant torque and a third-order model (the differential states being rotor speed and flux linkages) [4].

Moreover, it includes 22 DG units, of which 13 are 3-MVA synchronous generators and the remaining are 3.3-MVA Doubly Fed Induction Generators (DFIGs) [22]. The reactive power of each 3-MVA synchronous generator is adjusted to the value received from the DNV controller using a local proportional-integral control loop. The latter acts on the set-point of a voltage regulator (responding to faster changes). Similarly, the DFIGs operate in reactive power control mode, see [22], to meet the power requested by the DNV controller.

The combined transmission and distribution model includes 3108 buses, 20 large and 520 small synchronous generators, 600 motors, 360 DFIGs, 2136 voltage-dependent loads and 56 LTC-equipped transformers. This model was simulated with the RAMSES software developed at the University of Liège [23].

### B. DNV controller settings

Each of the 40 DNs is equipped with a separate DNV controller, detailed in Section II. This discrete-time controller

Table I  
OVERVIEW OF SIMULATED SCENARIOS

| Case | DN type | Stable | Contingency  | Section |
|------|---------|--------|--|---------|
| A1   | passive | yes    | outage of line 4061-4062   | V       |
| A2   | active  |        |  |         |
| B1   | passive | no     | 5-cycle short-circuit near bus 4032, cleared by opening line 4032-4042 | VI      |
| B2   | active  |        |  |         |
| B3   |         |        |  |         |
| C1   | passive | no     |  | VII     |
| C2   | active  |        |  |         |
| C3   |         |        |  |         |

is coupled with RAMSES from which it receives “measured” values, and to which it sends back adjusted DG unit set-points.

Measurements involve DG unit active/reactive powers and terminal voltages, as well as voltages at three load buses. The latter were selected so that no load is more than two branches away from a voltage monitored bus.

Measurement noise was simulated by adding a Gaussian random variable limited to  $\pm 0.01$  pu for voltages, and  $\pm 1\%$  of the DG maximum active and reactive powers.

The controller uses  $N_c = N_p = 3$  (unless  $N_p$  is increased to anticipate LTC actions, see [15]). The action period of each controller is constant but differs from one DN to another, with values between 10 and 15 s. As explained in [15], this includes a delay between the set-point adjustments and the collection of new measurements, a period of measurement sampling and the time required to solve the optimization.

The weight matrices  $\mathbf{R}$  and  $\mathbf{S}$  in (3) are diagonal; their non-zero elements are such that the “cost” for changing active powers is ten times higher than that of reactive powers, and the cost for relaxing voltage limits one hundred times higher.

The sensitivity matrices are computed off-line using data of the corresponding DN and are kept constant. For this calculation, the transmission grid is replaced by a Thévenin equivalent whose impedance is obtained from the short-circuit power at the corresponding DN connection point. Furthermore, it is assumed that the Thévenin impedance relates to the pre-fault configuration and is not updated after an outage in the TN. Indeed, updating the sensitivities with changes of this impedance entails passing information from TN to DN, which represents an additional complexity. The impact of this approximation is further assessed in the sequel.

### C. Overview of simulations

Table I shows the simulations performed in the following sections. These are divided into three groups of results, considering: stable cases, unstable cases, and unstable cases stabilized with the use of emergency control actions.

## V. RESULTS IN STABLE SCENARIOS

### A. Case A1

In this first scenario, the DNV controllers are not in service. The DG units operate with constant reactive powers and do not take part in voltage control. This leaves only the traditional voltage control by LTCs. Hence, the DNs are considered passive as in the first case of Section II.

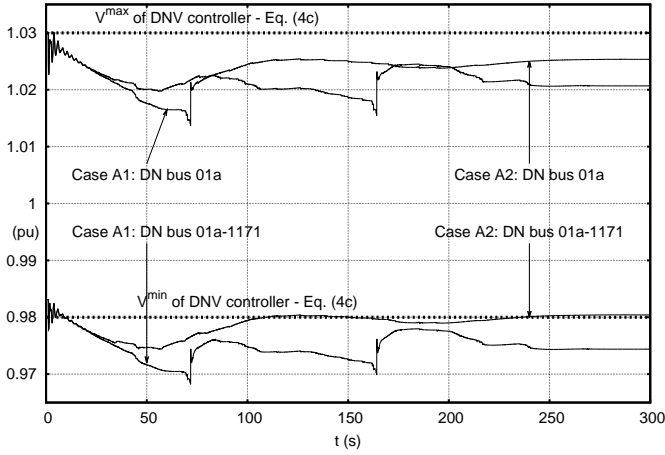


Figure 7. Cases A1 & A2: voltages at two DN buses

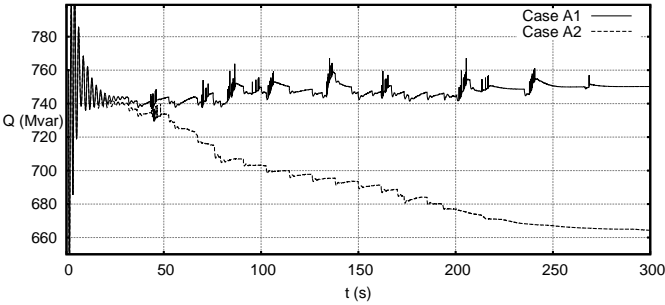


Figure 8. Cases A1 & A2: reactive power from TN to DNs

The long-term evolution of the system, until it returns to steady state is shown in Figs. 6 and 7. It is driven by the LTCs, in response to the voltage drops initiated by the line tripping. There are some 112 tap changes in all 40 DNs.

Figure 6 shows the TN voltage evolution at three representative buses of the Central area. The voltage at bus 1041 is the most impacted but remains above 0.985 pu. All DN voltages are successfully restored in their dead-bands by the LTCs, which corresponds to a stable evolution [5]. For instance, Fig. 7 shows the voltage evolution at two DN buses: 01a, controlled by an LTC with a [1.02 1.03] pu dead-band, and 01a-1171, located further away in the same DN.

### B. Case A2

The same disturbance as in Case A1 is considered, but the DNV controllers are now active. For simplicity, all components of  $V^{min}$  have been set to 0.98 pu and those of  $V^{max}$  to 1.03 pu. This interval encompasses all LTC deadbands, so that there is no conflict between an LTC and the DNV controller.

The corresponding TN and DN voltage evolutions can be found in Figs. 6 and 7, for easier comparison. With respect to Case A1, a steady state is reached at almost the same time, while the TN voltages are slightly higher. The voltages at DN buses not directly controlled by LTCs (such as 01a-1171 in Fig. 7) are restored above  $V^{min}$  by the DNV controller.

It is worth mentioning that the number of tap changes has decreased from 112 to 35, showing that the sharing of the control effort by active DNs reduces the wear of LTCs.

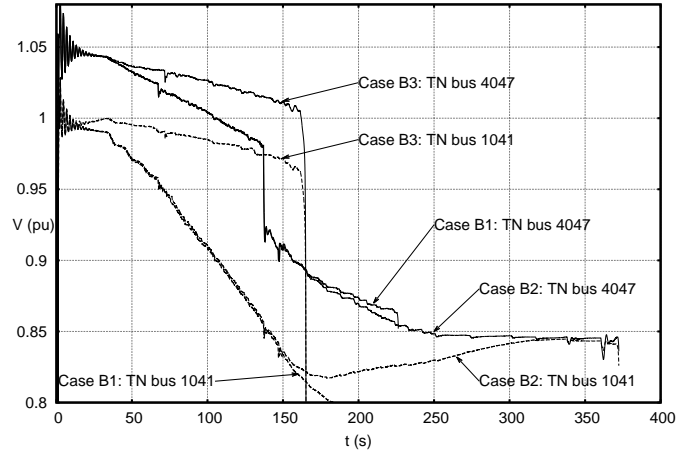


Figure 9. Cases B1, B2 & B3: voltages at two TN buses

The DN buses such as 01a-1171 in Fig. 7 have their voltages increased by the additional reactive power produced by the coordinated DG units. For instance, in Case A2 the DG unit participations decrease by almost 90 Mvar the net reactive power load seen by the TN (see fig. 8), which contributes to increasing TN voltages. This is the second benefit of active DN management.

Note, however, that a hidden effect of this load voltage increase is an increase of active and reactive powers of the voltage sensitive loads. While very moderate in this scenario, this effect will be predominant in the next ones.

## VI. RESULTS IN UNSTABLE SCENARIOS

### A. Case B1

The more severe disturbance of Case B is now considered.

Similarly to Case A1, the DN voltages are controlled by LTCs only. The voltage evolutions at two TN buses are shown in Fig. 9. The sustained voltage sag caused by the LTCs and OELs ends with a system collapse due to the loss of synchronism of machine g6 at  $t \simeq 225$  s. The maximum power that can be provided to loads is severely decreased by the initial line outage as well as cascading field current reductions due to seven OELs acting before  $t \simeq 147$  s. At the same time, the LTCs unsuccessfully attempt to restore DN voltages, which is impossible since load powers cannot be restored at their pre-disturbance values [5]. The static aspects of this mechanism were analysed in Section II-A.

### B. Case B2

As in Case A2, the DNV controllers are now active. Figure 9 shows, however, that their effect is merely to postpone system collapse by some 150 seconds. In the meantime, TN voltages stagnate at unacceptably low values (not to mention the likely disconnection of generators due to - non modeled - under-voltage protections). Figure 10 shows the voltage evolutions at DN buses located on the same feeder as buses 01a and 01a-1171, considered in Fig. 7. The DNV controllers respond tardily, when TN voltages are already low.

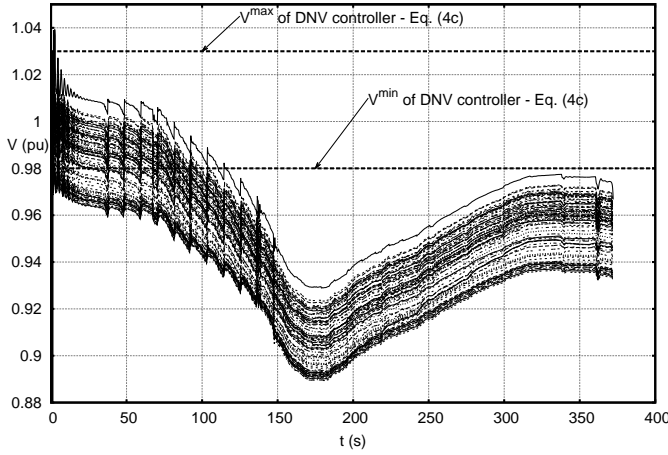


Figure 10. Case B2: voltages at various DN buses of the same feeder

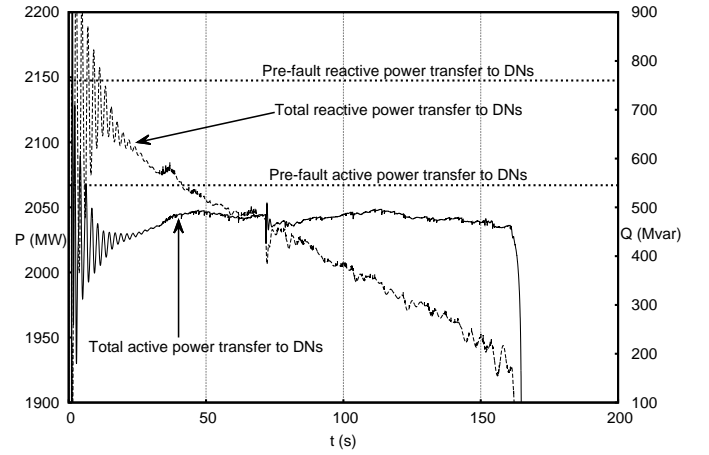


Figure 12. Case B3: total active and reactive power transfer from TN to DNs

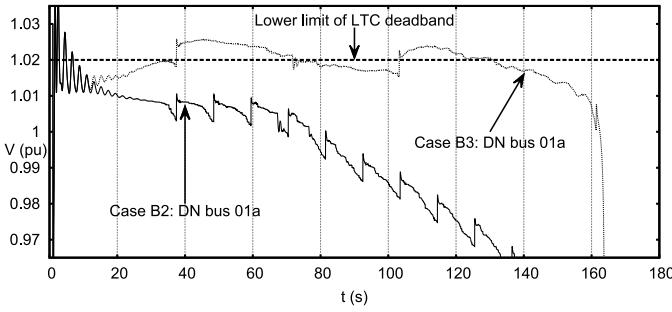


Figure 11. Cases B2 & B3: voltage at a DN bus controlled by an LTC

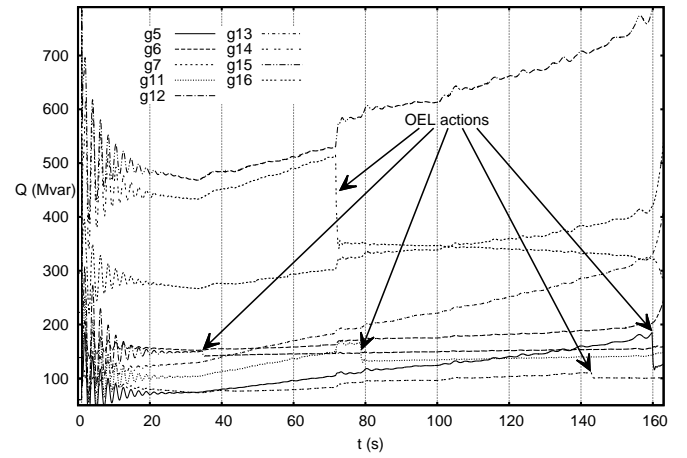


Figure 13. Case B3: reactive power produced by TN-connected generators

The explanation is found in the model used, more precisely the value of  $\Delta V_d$  in Eq. (2). The latter was chosen assuming normal voltage control at TN level, i.e. with the large generators holding their voltages. However, in Case B2, the effect of tap changes on DN voltages is very different, as illustrated in Fig. 11. In this figure, the solid line shows the evolution of the voltage at the DN bus controlled by a TN-DN transformer connected to bus 1041. The tap changes taking place at respectively  $t = 37, 48$  and  $59$  s, yield temporarily the expected DN voltage increases, but the latter are offset, in the following seconds, by the effects of LTCs acting in the other DNs. This is a feature of long-term voltage instability, analyzed in detail in [24]. Thus, the effective value of  $\Delta V_d$ , taking into account LTCs acting in other DNs, is actually close to zero. By relying on larger, optimistic values, each DNV controller overestimates the contribution of its LTC and, therefore, lacks responsiveness.

### C. Case B3

To make each DNV controller more responsive, one option is to ignore the contribution of the corresponding LTC, by removing the last term in Eq. (2). This is considered in Case B3, where LTCs are left to act as usual, but concurrently with the DNV controllers. The resulting voltage evolutions can be found in Figs. 9 and 11, while Fig. 12 shows the total active and reactive powers transferred from the TN to the DNs.

Since the DG units have their reactive power productions increased to correct DN voltages, the net reactive power load

seen by the TN decreases progressively, passing from 750 to 200 Mvar in 150 s. This results in TN voltages dropping significantly less than in Cases B1 and B2, until  $t \approx 150$  s (see Fig. 9). In principle, this reactive support could prevent voltage instability, but it is not sufficient in Case B3, where five OELs are activated successively. The limitations of generator reactive powers are identified in Fig. 13. At  $t \approx 165$  s, soon after the fifth OEL is activated, the system collapses with all generators in the Central and South areas, except g14, going out of step with the rest of the system.

This severe outcome is partly explained by the fact that the DNV controllers promptly restore voltages, and hence, load powers. Consequently, when generators connected to TN stop controlling their voltages, under the effect of OELs, they are facing a higher load power compared to Cases B1 and B2.

The restoration of DN voltages is illustrated by the dotted curve in Fig. 11. The voltage is boosted by the controller in significantly less time than with a traditional LTC, with the result that the LTC makes two tap changes only. The resulting, fast restoration of load active power is shown in Fig. 12, where the small, 25-MW non restored power is caused by the (intentional) voltage dead-bands of LTC and DNV controllers.

The overall effect of voltage control at DN level is to precip-

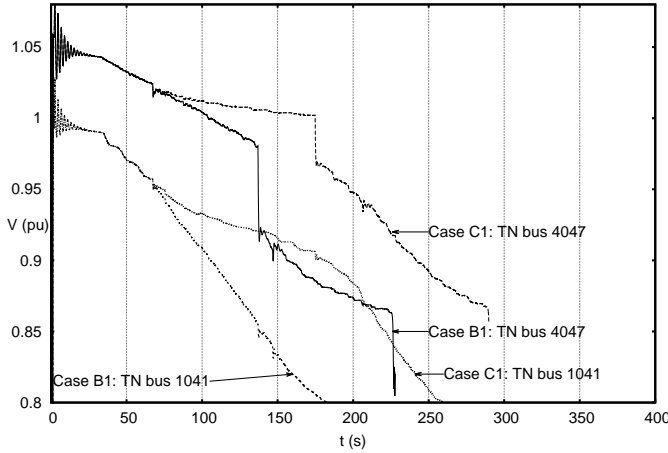


Figure 14. Cases B1 & C1: voltages at two TN buses

itate system collapse, while making the latter less predictable from the mere observation of voltages. From system operation viewpoint, this case is worse than Case B2. The static aspects of this behaviour were explained in Section II-B.

## VII. RESULTS WITH EMERGENCY SUPPORT FROM DISTRIBUTION

In this section, Case B is revisited assuming a remedial action to secure the system operation. This requires a timely detection of the emergency condition, which is first discussed.

### A. Emergency detection

The LIVES (standing for Local Identification of Voltage Emergency Situations) method of Ref. [24] detects the unsuccessful attempt of LTCs to restore their DN voltages. LIVES monitors each LTC independently. The absence of information exchange between substations is in agreement with the distributed DNV control structure considered in this study. Applied to the voltage evolution shown with solid line in Fig. 11, LIVES issues an emergency signal at  $t \simeq 70$  s (with some security margin against false alarms) [24].

As shown in Section VI-B, in Case B2, until the moment LIVES triggers an alarm, the contribution of the DNV controller is marginal. In Case B3, on the contrary, Fig. 11 shows that the DNV controller takes over from the LTC, acting more rapidly on the DG unit reactive powers. Observation of DN voltage restoration by LTCs, which is at the heart of LIVES, is no longer relevant, and emergency detection at DN level does not seem possible for Case B3. The alarm should come from the TN level, even if this entails information transfer.

The reactive reserve of the large, TN-connected generators make up an alternative alarm signal, combining simplicity with anticipation capability. It is quite common to have generator reactive power output measurements in the SCADA system of TN control centers. A comparison with capability curves can flag a generator that has switched under limit. In this study, it is assumed that the first three generator limitations shown in Fig. 13 will trigger the emergency signal at  $t \simeq 80$  s.

In the cases presented in this section both detection schemes have been used. First, in Cases C1 and C2, the detection

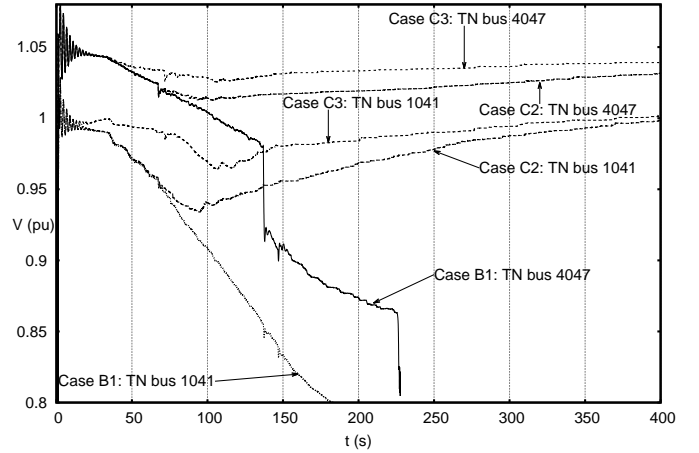


Figure 15. Cases B1, C2 & C3: voltages at two TN buses

method using LIVES has been used. Following, in Case C3, the detection method using an emergency signal triggered by the generators getting limited is used.

### B. Load Voltage Reduction

The remedial action considered in this study is a decrease of DN voltages exploiting sensitivity of load power to voltage. This effect strongly depends on the type of loads [4], [5], [12]. As long as a decrease in the voltage magnitude leads to decreased load consumption (in active and/or reactive power), the mechanism is beneficial to system stability. However, some loads (for instance induction motors and electronically controlled loads) have the tendency to rapidly restore their consumed power after a voltage decrease. Moreover, induction motors could eventually exhibit increased consumption when approaching their unstable region [4].

The voltage decrease  $\Delta V$  should be as large as possible while ensuring a minimum acceptable voltage at all DN nodes [12]. When implemented through LTC voltage decrease alone, this reduction is applied at only one point of the DN. This has led system operators to conservatively set  $\Delta V$  to 0.05 pu [4], [5]. On the other hand, acting on multiple DG units offers better controllability by adjusting DN voltages at multiple points. Therefore, more points of the DN have their voltages decreased while still remaining above the acceptable limit.

Moreover, as the LTC controllers involve mechanical components, their speed of action is limited and can be insufficient to counteract instability. Acting on DG units offers a significantly faster control of DN voltages.

### C. Case C1

This case involves the classical LTC voltage set-point reduction without any contribution by DG units. Thus, this scheme is to be compared to Case B1, from which it differs after  $t \simeq 70$  s, when the alarm from LIVES is issued. At that time, the LTC voltage set-points are decreased by  $\Delta V = 0.05$  pu.

Figure 14 shows the voltage evolution at two TN buses. It can be seen that the amount of load decrease is not enough to stabilize the system. Further tests showed that  $\Delta V = 0.08$  pu

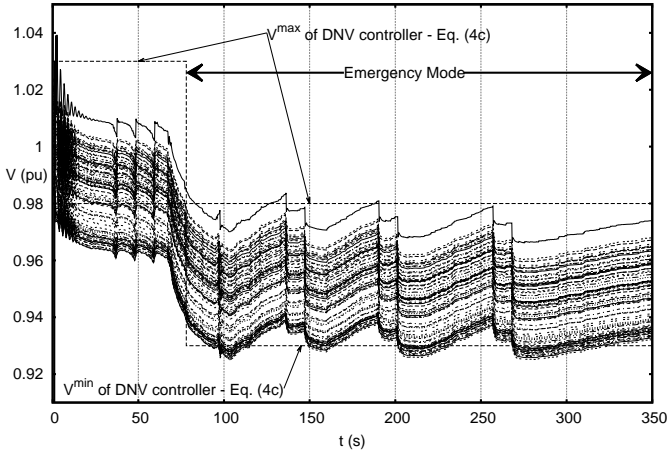


Figure 16. Case C2: voltages at various DN buses of the same feeder

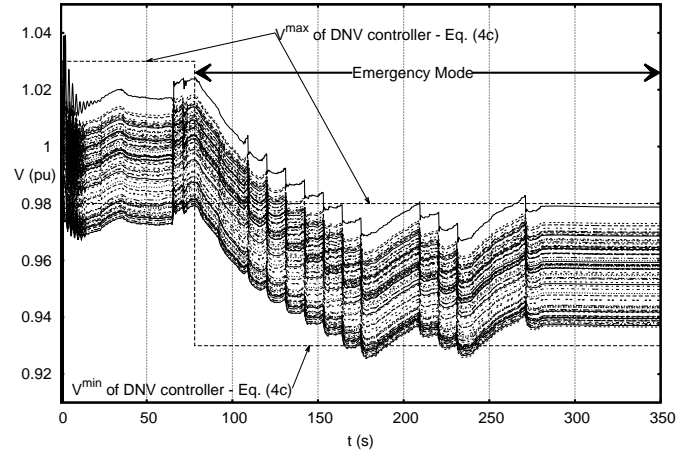


Figure 18. Case C3: voltages at various DN buses of the same feeder

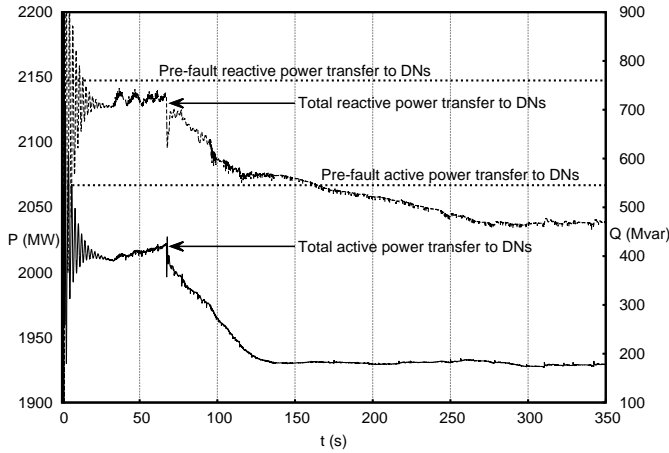


Figure 17. Case C2: total active &amp; reactive power transfer from TN to DNs

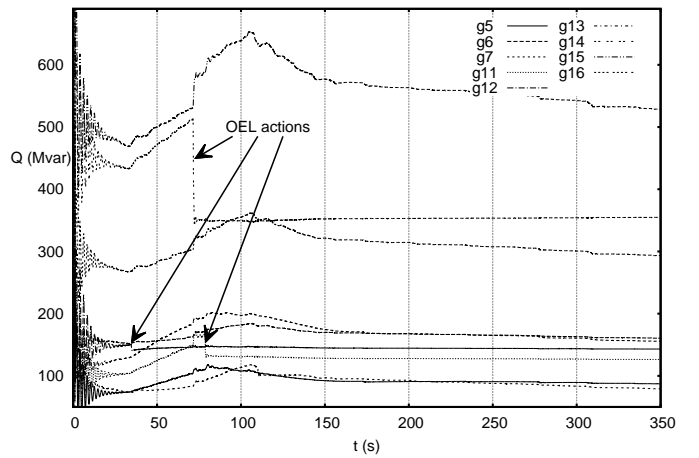


Figure 19. Case C3: reactive power produced by TN-connected generators

would be needed. However, in that case, several DN bus voltages are unacceptable, lower than 0.90 pu.

#### D. Case C2

Case C2 is to be compared with Case B2, from which it differs after  $t \simeq 70$  s, when the alarm from LIVES is issued. At that time, the above mentioned  $\Delta V$  corrections are applied. While in the unstable case B2, LTCs were unable to restore DN voltages, in this case, they contribute, together with DNV controllers, to depressing the DN voltages.

Voltage evolutions at TN buses are shown in Fig. 15, together with those of the uncontrolled Case B1, for comparison purposes. The TN voltages are smoothly stabilized.

Figure 16 shows the corresponding voltage evolutions in the DN previously considered in Fig. 10, together with the changing  $V^{\min}$  and  $V^{\max}$  limits. It is seen that the DN voltages are promptly brought within the new desired ranges.

The voltage reduction causes the decrease of active and reactive power transfer from the TN to DNs, as shown in Fig. 17. As explained in Section IIB, the reactive power transferred between the TN and DNs varies with the reactive power produced by DG units, the reactive power consumed by loads, and the network losses. First, the DG units are

directed by the DNV controllers to reduce and maintain the DN voltages within the emergency limits. To achieve this, they decrease their reactive power productions. Then, the reduced DN voltages lead to decreased reactive power consumption by the loads and decreased losses. In the system studied, the benefit brought by the load decrease outweighs the negative impact of the reduced reactive support from DG units. Thus, the restored power point is moved as shown in the left sub-plot of Fig. 3, entering the feasible region.

#### E. Case C3

Case C3 is to be compared with Case B3, from which it differs after  $t \simeq 80$  s, when the generator limitation alarm is received. In both cases, the DNV controllers operate concurrently with the LTCs, the last term in (2) being ignored.

The TN voltage evolutions are provided in Fig. 15, for comparison with Cases B1 and C2. The system is stabilized at similar voltage values.

Figure 18 shows the voltage evolutions in the DN considered in Figs. 10 and 16. In response to the initial disturbance, the DNV controller of concern has almost restored the DN voltages in the original [0.98 1.03] pu interval when the

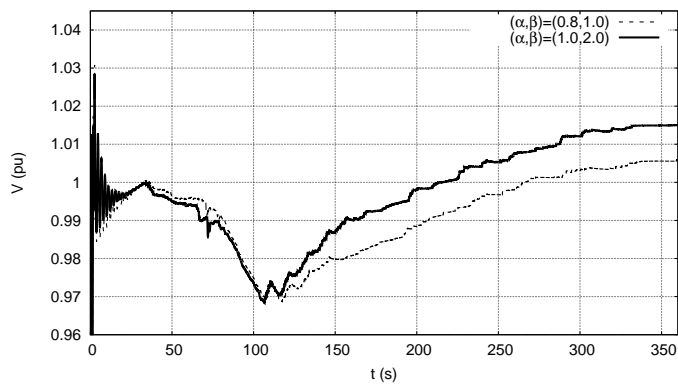


Figure 20. Case C3: voltage at a TN bus with two different load model parameter pairs; voltage reduction  $\Delta V = -0.05$  pu

emergency alarm is received. After the alarm it takes about the same time to steer the voltages in the shifted interval.

The evolution of reactive powers of TN-connected generators for Case C3 is shown in Fig. 19. It can be seen that no further generator limitation takes place after  $t = 80$  s, in contrast to Case B3 where the system eventually collapses after the successive field current limitations of generators g5 and g6, as shown in Fig. 13. Furthermore, the non-limited generators are relieved, as shown by Fig. 19.

To assess the robustness of the scheme to delays in emergency detection signals, three cases were considered, each with an additional delay of 30 s added to the original alarm time of 80 s. With delays up to 60 s (i.e., with an emergency alarm up to  $t = 140$  s), the system can be saved. This is made possible by the fast response of DG units steered by the DNV controllers. Expectedly, there exists a no-return point: if the alarm is received later than 145 s, the system can not be saved.

#### F. Sensitivity of method to load types

The emergency technique proposed in this paper exploits the reduction of load consumption when voltages are decreased. Thus, the sensitivity of loads towards voltage variations is critical to its success. This sensitivity is taken into account through the parameters  $\alpha$  and  $\beta$ , used in the load model (5).

These parameters are selected according to the mixture of loads present in the system. An indicative list can be found in [4], [5]. When the induction motors are modelled explicitly, such as in the test system used in this paper, the values  $(\alpha, \beta) = (1.0, 2.0)$  are frequently used.

These load model parameters determine the load power decrease for a given voltage reduction. Figure 20 shows the voltage at a TN bus in Case C3 ( $\Delta V = -0.05$  pu), with two different sets of parameters. The first pair  $(\alpha, \beta) = (0.8, 1.0)$  is an extreme case, where the loads have very low sensitivity to voltage; while the second, is the one used in this paper. It can be seen that, even though in both cases the system is saved, with more sensitive loads the voltage recovers a little faster to a higher value.

Furthermore, a parametric study can be performed to check the effectiveness of the method as a function of the load model parameters and the emergency voltage reduction ( $\Delta V$ ). Such

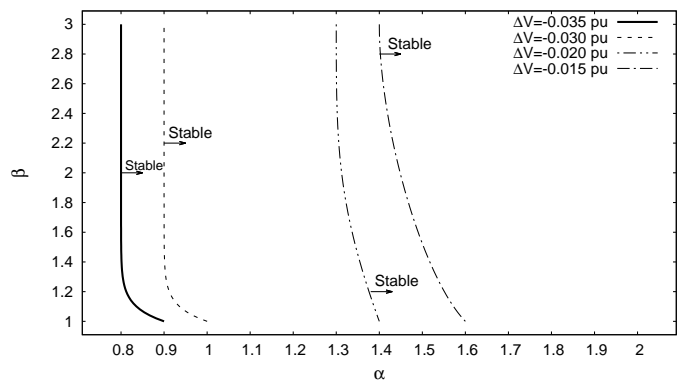


Figure 21. Case C3: regions of successful stabilization in the  $(\alpha, \beta)$  space, for various voltage reduction values  $\Delta V$

a study has been performed on Case C3. The simulation was considered for several values of  $\Delta V$  ( $-0.05, \dots, -0.01$  pu) and using a wide range of  $\alpha$  ( $0.8, \dots, 2.0$ ) and  $\beta$  ( $1.0, \dots, 3.0$ ) parameter pairs. For  $\Delta V = -0.05$  pu (used in the paper) and  $\Delta V = -0.04$  pu, the system is stabilized for all  $(\alpha, \beta)$  pairs. For smaller voltage reduction, Fig. 21 shows the values for which the system is saved.

According to the plot, in this test system, active power reduction is more effective than its reactive power counterpart. For less sensitive active power loads (lower  $\alpha$  values), voltage instability completely depends on  $\alpha$  irrespective of the  $\beta$  value. As active power load is more sensitivity to voltage,  $\beta$  starts to have some more importance. Moreover, it is confirmed that, as loads get more voltage sensitive (higher  $\alpha$  and  $\beta$  values), a smaller  $\Delta V$  is sufficient to stabilize the system.

## VIII. CONCLUSION

This paper has reported on simulations of a large-scale test system including one TN and multiple DNs. The latter are assumed to be active by controlling the reactive power of DG units, with the aim of keeping DN voltages within a desired range. The DNs are controlled independently of each other, and of the TN. In this study, a specific MPC-based scheme was considered. However, the results are representative of future smart grids in which DG units will contribute to regulating voltages at other buses than the one controlled by the LTC.

In normal operating conditions, the case study shows some benefits of DNV control after a disturbance affecting the TN: (i) by increasing the DG unit reactive powers to support DN voltages, the power factor at the TN/DN connection point is improved; (ii) the number of LTC steps is decreased.

On the contrary, in long-term voltage instability scenarios:

- DNV control is impacted by the growing weakness of the TN system which behaves very differently from what is assumed in the DNV control scheme, set up for “normal” conditions. The main discrepancy stems from LTCs unable to restore DN voltages as expected;
- DNV control may, in turn, impact system dynamics. This is the case when DG units are controlled concurrently (and not in complement) to LTCs to restore the DN voltages, and hence the load powers. This fast load power

restoration may precipitate system collapse, making the situation more severe than with classical LTC control.

On the other hand, DNV control can contribute to corrective actions against voltage instability by decreasing the DN voltages, thereby reducing the power consumed by loads, through the reduction of reactive power production of DG units. The above action can be triggered:

- either locally, observing the unsuccessful attempt of the LTC to restore its DN voltage, when the DNV controller is designed to complement LTC operation;
- or centrally, from an alarm signal issued at TN level, when the DNV controller is set to operate concurrently with the LTC.

## REFERENCES

- [1] J. P. Lopes, N. Hatzargyriou, J. Mutale, P. Djapic, and N. Jenkins, "Integrating distributed generation into electric power systems: A review of drivers, challenges and opportunities," *Electric Power Systems Research*, vol. 77, no. 9, pp. 1189 – 1203, 2007.
- [2] A. A. Bayod-Rújula, "Future development of the electricity systems with distributed generation," *Energy*, vol. 34, no. 3, pp. 377–383, 2009.
- [3] G. Joos, B.-T. Ooi, D. McGillis, F. Galiana, and R. Marceau, "The potential of distributed generation to provide ancillary services," in *Proc. IEEE PES 2000 Summer Meeting*, 2000, pp. 1762–1767.
- [4] C. W. Taylor, *Power System Voltage Stability*. Mc Graw Hill, 1994.
- [5] T. Van Cutsem and C. Vournas, *Voltage Stability of Electric Power Systems*. Springer, 1998.
- [6] ENTSO-E, "Network code on demand connection," Tech. Rep. 1-63, Dec 2012. [Online]. Available: <https://www.entsoe.eu>.
- [7] G. Valverde and T. Van Cutsem, "Control of dispersed generation to regulate distribution and support transmission voltages," in *Proc. IEEE PES 2013 PowerTech*, June 2013.
- [8] C. Vournas and M. Karystianos, "Load tap changers in emergency and preventive voltage stability control," *IEEE Transactions on Power Systems*, vol. 19, no. 1, pp. 492–498, 2004.
- [9] C. Vournas, A. Metsiou, M. Kotlida, V. Nikolaidis, and M. Karystianos, "Comparison and combination of emergency control methods for voltage stability," in *Proc. IEEE PES 2004 General Meeting*, 2004, pp. 1799–1804 Vol.2.
- [10] I. Hiskens and B. Gong, "Voltage stability enhancement via model predictive control of loads," in *Intelligent Automation and Soft Computing*, vol. 12, 2006.
- [11] C. Crider and M. Hauser, "Real time T&D applications at Virginia Power," *IEEE Computer Applications in Power*, vol. 3, no. 3, pp. 25–29, 1990.
- [12] Z. Wang and J. Wang, "Review on implementation and assessment of conservation voltage reduction," *IEEE Transactions on Power Systems*, vol. 29, no. 3, pp. 1306–1315, May 2014.
- [13] I. Dobson and L. Lu, "New methods for computing a closest saddle node bifurcation and worst case load power margin for voltage collapse," *IEEE Transactions on Power Systems*, vol. 8, no. 3, pp. 905–913, Aug 1993.
- [14] M. Biserica, B. Berseneff, Y. Besanger, and C. Kieny, "Upgraded coordinated voltage control for distribution systems," in *Proc. IEEE PES 2011 PowerTech*, June 2011.
- [15] G. Valverde and T. Van Cutsem, "Model predictive control of voltages in active distribution networks," *IEEE Transactions on Smart Grid*, vol. 4, no. 4, pp. 2152–2161, Dec. 2013.
- [16] M. Moradzadeh, R. Boel, and L. Vandevelde, "Distributed communication-based model predictive control for long-term voltage instability," in *Proc. IEEE PES 2013 Power and Energy Engineering Conference (APPEEC)*, Dec 2013.
- [17] —, "Voltage coordination in multi-area power systems via distributed model predictive control," *IEEE Transactions on Power Systems*, vol. 28, no. 1, pp. 513–521, Feb 2013.
- [18] J. M. Maciejowski, *Predictive Control With Constraints*. Prentice-Hall, 2002.
- [19] G. Valverde and J. Orozco, "Reactive power limits in distributed generators from generic capability curves," in *Proc. IEEE PES 2014 General Meeting*, 2014.
- [20] S. Engelhardt, I. Erlich, C. Feltes, J. Kretschmann, and F. Shewarega, "Reactive power capability of wind turbines based on doubly fed induction generators," *IEEE Transactions on Energy Conversion*, vol. 26, no. 1, pp. 364–372, March 2011.
- [21] T. Van Cutsem and L. Papangelis, "Description, modeling and simulation results of a test system for voltage stability analysis," University of Liège, Internal report, Nov. 2013. [Online]. Available: <http://hdl.handle.net/2268/141234>
- [22] A. Ellis, Y. Kazachkov, E. Muljadi, P. Pourbeik, and J. Sanchez-Gasca, "Description and technical specifications for generic WTG models: A status report," in *Proc. IEEE PES 2011 Power Systems Conference and Exposition (PSCE)*, March 2011.
- [23] P. Aristidou, D. Fabozzi, and T. Van Cutsem, "Dynamic simulation of large-scale power systems using a parallel Schur-complement-based decomposition method," *IEEE Transactions on Parallel and Distributed Systems*, vol. 25, no. 10, pp. 2561–2570, Oct 2014.
- [24] C. Vournas and T. Van Cutsem, "Local identification of voltage emergency situations," *IEEE Transactions on Power Systems*, vol. 23, no. 3, pp. 1239–1248, 2008.

**Petros Aristidou** (S'10) obtained his Diploma in Electrical and Computer Engineering from the National Technical University of Athens, Greece, and his Ph.D. in Electrical Power Systems from the University of Liège, Belgium, in 2010 and 2015, respectively. He is currently a Postdoctoral Researcher at the Swiss Federal Institute of Technology in Zurich (ETHZ). His research interests include power system dynamics, control, and simulation. In particular, investigating the development and use of high performance computational tools in future power systems.

**Gustavo Valverde** (S'08-M'12) obtained the B.Sc. degree in Electrical Engineering from the University of Costa Rica in 2005 and the M.Sc. and Ph.D. in Electrical Power Systems from the University of Manchester, UK, in 2008 and 2012, respectively. From 2012 to early 2013 he worked as postdoctoral researcher at the University of Liège, Belgium. Currently he is an Associate Professor at the University of Costa Rica. His research interests include monitoring of power systems, optimization methods, power system modeling and analysis, voltage stability and voltage control of distribution networks.

**Thierry Van Cutsem** (F'05) graduated in Electrical-Mechanical Engineering from the University of Liège, Belgium, where he obtained the Ph.D. degree and he is now adjunct professor. Since 1980, he has been with the Fund for Scientific Research (FNRS), of which he is now a Research Director. His research interests are in power system dynamics, stability, security, monitoring, control and simulation. He has been working on voltage stability in collaboration with transmission system operators from France, Canada, Greece, Belgium and Germany. He is Past Chair of the IEEE PES Power System Dynamic Performance Committee.